INTERNATIONAL JOURNAL FOR NUMERICAL METHODS IN FLUIDS
Int. J. Numer. Meth. Fluids (2016)
Published online in Wiley Online Library (wileyonlinelibrary.com). DOI: 10.1002/fld.4357

Improving the convergence behaviour of a fixed-point-iteration solver for multiphase flow in porous media

P. Salinas[1,2,*,†], D. Pavlidis[1,2], Z. Xie[1,2], A. Adam[1,2], C. C. Pain[1,2] and M. D. Jackson[1]

[1]*Novel Reservoir Modelling and Simulation Group, Department of Earth Science and Engineering, Imperial College London, London, UK*
[2]*Applied Modelling and Computation Group, Department of Earth Science and Engineering, Imperial College London, London, UK*

SUMMARY

A new method to admit large Courant numbers in the numerical simulation of multiphase flow is presented. The governing equations are discretized in time using an adaptive θ-method. However, the use of implicit discretizations does not guarantee convergence of the nonlinear solver for large Courant numbers. In this work, a double-fixed point iteration method with backtracking is presented, which improves both convergence and convergence rate. Moreover, acceleration techniques are presented to yield a more robust nonlinear solver with increased effective convergence rate. The new method reduces the computational effort by strengthening the coupling between saturation and velocity, obtaining an efficient backtracking parameter, using a modified version of Anderson's acceleration and adding vanishing artificial diffusion. © 2016 The Authors. *International Journal for Numerical Methods in Fluids* Published by John Wiley & Sons Ltd.

Received 29 January 2016; Revised 28 September 2016; Accepted 25 November 2016

KEY WORDS: nonlinear solvers; fixed point iteration; multiphase flow; porous media; implicit time stepping; Darcy flow

1. INTRODUCTION

Many porous media flow problems involve highly heterogeneous domains including features such as fractures, which result in a wide range of element sizes and hence local Courant numbers [1]. Moreover, the use of dynamic mesh adaptivity to capture sharp saturation fronts when one fluid phase displaces another can also introduce very small elements [1, 2]. It is desirable that computational efficiency should not be compromised by having the time step limited by a few very large values of local Courant number. Numerical simulations with Courant numbers greater than unity do not always yield poor solutions [3].

Newton methods have been traditionally used to solve porous media multiphase flows [4, 5]. Likewise, the fixed point method of Anderson (termed here the FPMA) has also been used [1, 6–8] because of its simplicity, as it solves the discretized equations directly and because of its fewer requirements to achieve convergence [9].

Convergence of the solver is never guaranteed when dealing with a nonlinear system of equations. Both local and global convergence must be considered. In the former, the initial guess must be close to the solution, while in the latter, the initial guess can be far from the solution [10]. Many methods have been developed in order to obtain global convergence, such as the trust region method and the backtracking method [10, 11]. In this paper, a modification of the FPMA with acceleration that

*Correspondence to: P. Salinas, Novel Reservoir Modelling and Simulation Group, Department of Earth Science and Engineering, Imperial College London, London, UK.
†E-mail: pablo.salinas@imperial.ac.uk

allows large Courant numbers is presented. The work is motivated by the fact that the use of a simple FPMA is not enough to achieve convergence when dealing with large local Courant numbers.

The approach presented in this paper is based on four main ideas. First, a nested and cheaper FPMA is performed in order to accelerate the convergence of the nonlinear solver. Second, a more robust convergence is achieved by using backtracking techniques. Third, the convergence rate is increased using acceleration techniques based on Anderson's method [6]. Fourth, the convergence and convergence rate are increased through the use of artificial diffusion that vanishes when the solution has converged. These methods create a very efficient, more robust nonlinear solver that is able to solve for very large Courant numbers using few iterations.

2. GOVERNING EQUATIONS

The discretization used is presented in [1] and in [8]; here, only a summary of the equations is presented. Darcy's law for multiphase flow can be written as

$$\underline{\underline{\sigma}}_{\alpha}\mathbf{u}_{\alpha} = -\nabla p + \mathbf{s}_{u\alpha}, \tag{1}$$

where $\mathbf{u}_{\alpha}$ is the phase saturation-weighted Darcy velocity of phase α, p is the pressure of the system and $\mathbf{s}_{u_{\alpha}}$ is a source term, which may include gravity. $\underline{\underline{\sigma}}_{\alpha}$ is defined as

$$\underline{\underline{\sigma}}_{\alpha} = \mu_{\alpha} S_{\alpha} \left(\mathcal{K}_{r_{\alpha}}\mathbf{K}\right)^{-1}, \tag{2}$$

where $\mathbf{K}$ is the permeability tensor, and $\mathcal{K}_{r_{\alpha}}$, μ_{α} and S_{α} are the relative permeability, viscosity and saturation of phase α, respectively.

The saturation equation assuming incompressible and isothermal flow can be written as

$$\phi\frac{\partial S_{\alpha}}{\partial t} + \nabla\cdot\left(\mathbf{u}_{\alpha}S_{\alpha}\right) = s_{cty,\alpha}, \tag{3}$$

where ϕ is the porosity and s_{cty} is a source term.

To close the system of equations, the saturation is constrained by

$$\sum_{\alpha=1}^{n} S_{\alpha} = 1, \quad \forall\, n, \tag{4}$$

where n is the number of phases.

The spatial discretization considered in this paper is based on the control volume finite element method [1, 8, 12–14] in which the velocity and pressure are discretized using finite elements, and saturation and other conserved quantities are discretized using the control volumes. However, the method reported is independent of the spatial discretization scheme. Time is discretized using an implicit Θ-method, where Θ smoothly varies between 0.5 (Crank–Nicholson) and 1 (implicit Euler) based on a total variation diminishing criterion (see [15] for more details). This method guarantees that the time-discretization scheme is unconditionally stable for any time step, making the nonlinear solver the only limiting factor for the time step size.

3. A RELAXED TWO-FIXED POINT ITERATION SOLVER WITH ACCELERATION

To solve the nonlinear system of equations formed by Eqs (1), (3) and (4), a FPMA method is considered. The usual FPMA workflow for this system consists of first estimating a pressure solution from a saturation estimation, that is, the saturation estimation is used to calculate $\underline{\underline{\sigma}}$. Next, an estimate for velocity is obtained from the pressure, and finally, the saturation is updated. The solver iterates until a certain pre-defined saturation tolerance is reached or a maximum number of iterations are performed. Here, a modified approach is considered.

DOI: 10.1002/fld

According to [16], the main source of nonlinearity is the saturation equation (Eq. (3)) arising from the nonlinear relationships between relative permeability and saturation and (when included) capillary pressure and saturation, which result in a nonlinear relationship between fluid phase velocity and saturation. Thus, as shown in [5] for Newton solvers, only an extra step is required in order to stabilize the equations and increase the resilience and convergence of the nonlinear solver. Likewise, here, an extra step is added in the FPMA procedure. In this step, after calculating the saturation field, a solution is sought in a trust region by forcing the solution to fulfil the physical restrictions of the problem. Thus, the saturation field obtained after solving Eq. (3) is truncated to be within physical values. The truncation does not affect conservation of mass so long as the nonlinear solver achieves convergence, in which case no truncation is necessary because the values obtained are physically plausible.

The method outlined previously involves four modifications to the common FPMA method that can be applied independently. Each of these modifications are described in the following sections, and the overall algorithm is presented in Figure 1.

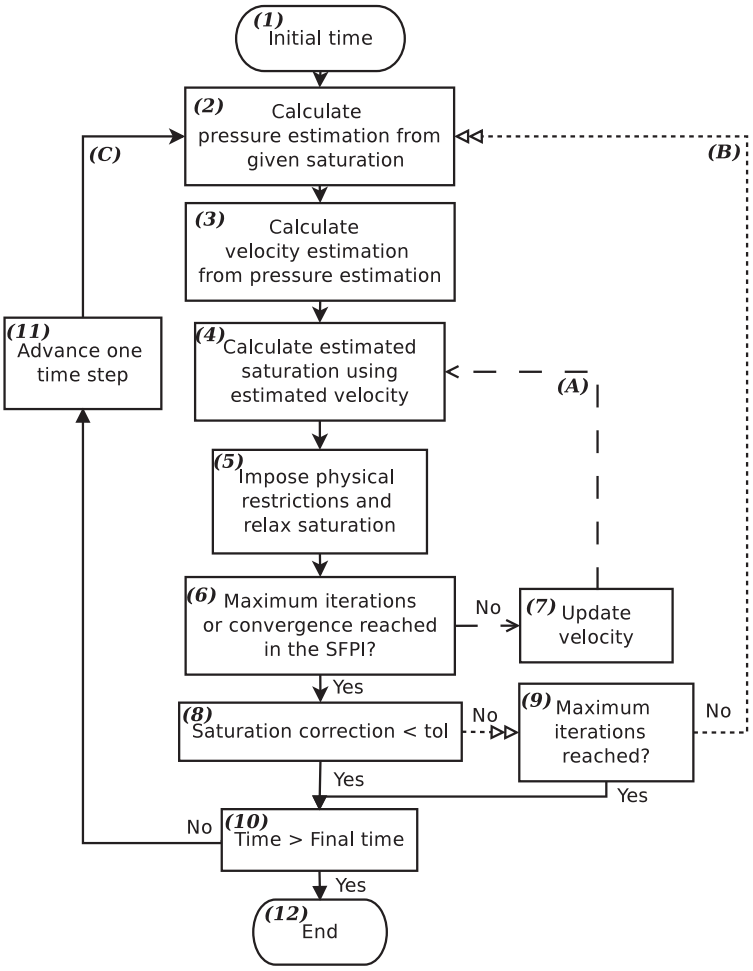

Figure 1. Flow chart showing the steps of the algorithm. There are three main loops in total. The solid lines denote the time loop. The dotted lines denotes the fixed point iteration method, which is used to solve the nonlinear system of equations. The dashed lines denote the saturation fixed point iteration, which is used to accelerate the fixed point method of Anderson.

DOI: 10.1002/fld

3.1. Saturation fixed point iteration

In porous media flow, the pressure field change is slower than the saturation field, and this feature of the solution has been used to admit Courant numbers over unity using implicit pressure explicit saturation formulations [17]. Here, an equivalent approach is considered in order to accelerate the convergence. Recalculating $\underline{\underline{\sigma}}_{\alpha}$ with the new estimation of the saturation, S'_k, provides a good approximation to recalculate a new velocity estimation without recalculating the pressure field. This implies that an inner FPMA can be performed in order to increase the convergence speed of the nonlinear solver.

Figure 1 shows the flow diagram of the proposed nonlinear solver. Three loops are considered. The solid line is the time loop (Figure 1 line (C)). The dotted-line is the classical FPMA loop (Figure 1 line (B)). The dashed-line (Figure 1 line (A)) is the inner FPMA loop proposed in this subsection, whose computational cost is approximately one-third of a conventional FPMA (this cost has been obtained by profiling the code for several cases). This latter iterative process only loops over the saturation. It is denoted as the saturation fixed point iteration (SFPI).

3.2. Relaxation parameter based on the history of convergence

A relaxation parameter (φ) can be used to increase the convergence of a solver [10]; moreover, for nonlinear solvers, like in the Newton solver with relaxation, it is a common procedure to obtain global rather than local convergence [18]. Thus, a relaxation method is considered here to improve the convergence of the FPMA. This is implemented after obtaining the saturation field (Figure 1 box (5)). The method is based on weighting the new guess of the field obtained after solving the equations with the value of the field in the previous iteration of the solver. In the case of the proposed nonlinear solver, the new guess of the saturation field is obtained using

$$S'_k = \varphi S_k + (1-\varphi) S_{k_1}, \tag{5}$$

where S_k is the value of saturation obtained at this SFPI, S_{k_1} is the saturations obtained in the previous SFPI, φ is the relaxation parameter and S'_k is the new estimation of the saturation.

Some authors have calculated the relaxation parameter, φ, in advance based on information about the flow [5]. Other options are based on exploring the different residuals obtained without updating the solution, to finally calculate the optimal parameter and then update the solution [10]. Here, a similar approach to this latter option is considered, with the difference that the solution is always updated.

At the beginning of a SFPI, the relaxation parameter is set to the value prescribed by the user. Within the SFPI, φ is calculated as the value that yields the best convergence ratio reducing the residual of the saturation. To this end, the last three values of the ratio of convergence of the residual are stored together with their corresponding relaxation parameter φ. A second-order system is created, and an optimal φ is calculated [10]. However, when no data are available or no minima can be obtained, the algorithm calculates φ solely based on the last value and its consequent convergence ratio. φ is increased if the method is converging and decreased otherwise. This guarantees that the algorithm explores the whole range of possible values for φ, between a maximum of 1 and a minimum value, 0.1 is recommended in [10] to find the most efficient value of φ. However, the most efficient value for the current iteration is not necessarily optimal for future iterations, so a new value is found for each iteration.

3.3. Acceleration of the nonlinear solver

Due to the slow convergence of the FPMA, [6] proposed an acceleration method in which the new guess is relaxed using previous estimations (Figure 1 box (5)). To this end, an optimal relaxation parameter is calculated for each previous estimation, which requires an optimization system to be created and solved. Here, a modified Anderson acceleration method is considered. Instead of using a different relaxation parameter for each previous estimation, the weighting of the previous estimations is solely based on the single relaxation parameter, φ, introduced previously, meaning it is not necessary to solve an optimization system.

DOI: 10.1002/fld

After solving Eq. (3), the saturation is relaxed using the last two values of saturation inside the SFPI. The new saturation is obtained using

$$S'_k = \varphi S_k + (1-\varphi)S_{k_1} + (1-\varphi)^{(\beta+1)}\varphi(S_{k_2} - S_{k_1}), \tag{6}$$

where S_{k_2} is the saturation estimate obtained in the previous SFPI to S_{k_1}. β is the exponent that controls the relative importance of S_{k_1} and S_{k_2} depending on the relaxation parameter φ.

For values of β below 0.4, the relative importance of S_{k_2} is increased over S_{k_1} (Figure 2 (a)); for values of β above 0.4, S_{k_2} is always below S_{k_1} (Figure 2 (b)), and as the value of β increases, the importance of S_{k_2} decreases (Figure 2 (c)). The shape of the curve formed from the weight of S_{k_2} (Figure 2) is asymmetric, being higher for smaller values of φ, when convergence is slow and the system is more likely to be oscillating, than for high values of φ when the system is converging well and no acceleration is required. Equation (6) guarantees consistency in the solution because the sum of all the contributions to the final solution is 1. Equation (6) also limits the contribution of S_{k_2} in the solution, which is a desired property as acceleration techniques can lead to divergence [7].

To increase robustness and avoid extra iterations, we use Eq. (5) for the final saturation update to ensure that the terms $(1-\varphi)^{(\beta+1)}$ and $(S_{k_2} - S_{k_1})$ do not contribute to the calculated saturation. One extra SFPI using Eq. (5) is performed.

3.4. Vanishing artificial diffusion in the saturation equation

The introduction of artificial diffusion is a well-known method to increase the stability of the numerical discretizations. However, the final solution obtained contains non-physical diffusion that modifies the results.

Here, an artificial diffusion is introduced, which depends on the difference of the saturation between two iterations of the nonlinear solver, so the artificial diffusion becomes zero when convergence is achieved (this step is performed when calculating the saturation, Figure 1 box (4)). In this way, the artificial diffusion is introduced only in regions of the domain where convergence is difficult. Moreover, the amount of artificial diffusion varies depending on the difficulty of convergence in the different regions of the domain.

Equation (3) is modified in order to add the artificial diffusion term

$$\phi\frac{\partial S_{k\alpha}}{\partial t} + \nabla\cdot(\mathbf{u}_\alpha S_{k\alpha} - \kappa\nabla(S_{k\alpha} - S_{k'\alpha})) = s_{cty,\alpha}, \tag{7}$$

where κ is the over-relaxation term that controls the amount of artificial diffusion and k is the inner iteration number. Thus, $S_{k'\alpha}$ is the saturation of phase α obtained at the previous SFPI (or FPMA if no SFPI is performed).

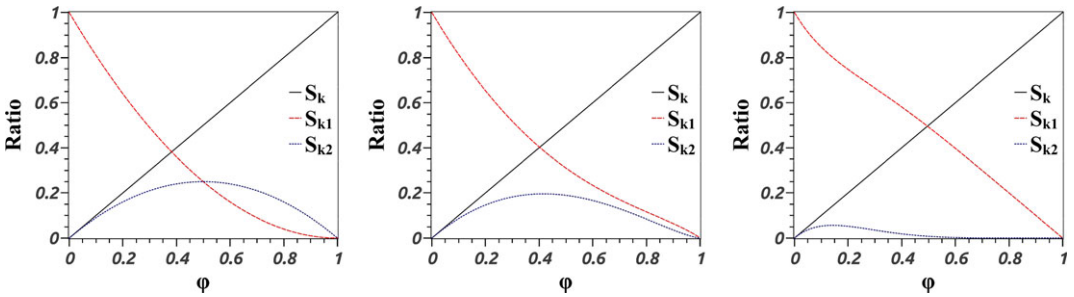

(a) $\beta = 0$ (b) $\beta = 0.4$ (c) $\beta = 10$

Figure 2. Weight of the different saturations, S_{k_i}, used to obtain the new S'_k depending on the relaxation parameter φ for different values of β. (a) Shows a big importance of S_{k_2}, even more important than S_{k_1}. (b) S_{k_2} is always less important than S_{k_1}. (c) S_{k_2} is barely considered. [Colour figure can be viewed at wileyonlinelibrary.com]

DOI: 10.1002/fld

Note that this method is completely independent of the nonlinear solver considered to solve the system of equations. The value of κ is recommended to be selected so a Peclet-like number, defined as

$$P_e = \frac{|\nabla p|}{\kappa l}, \tag{8}$$

where l is the characteristic length (e.q. element length) and ∇p, the gradient of pressure, is always > 10, that is, the artificial diffusion introduced per element is at least one order of magnitude smaller than the viscous effects (the numerator in Eq. (8)). It is important not to deviate the nonlinear solver too far from the correct path to the solution, because that can lead to more iterations to achieve convergence.

4. RESULTS

The method presented here is tested for three different test cases numbered 4.1–4.3. In all of them, we simulate two-phase immiscible flow in which one fluid phase displaces another fluid phase in a porous medium. To obtain the relative permeability for all the test cases, the Brooks–Corey model [19] is used:

$$k_{rw}\left(S_w\right) = \left(\frac{S_w - S_{wirr}}{1 - S_{wirr} - S_{nwr}}\right)^{n_w}, \tag{9}$$

$$k_{rw}\left(S_w\right) = \left(\frac{S_{nw} - S_{nwr}}{1 - S_{wirr} - S_{nwr}}\right)^{n_{nw}}, \tag{10}$$

where S_w and S_{nw} are the wetting and non-wetting phase saturations, S_{wirr} and S_{nwr} are the irreducible wetting and non-wetting phase saturations, and n_w and n_{nw} are the exponents for the wetting and non-wetting phases, respectively. The exponents of the relative permeability model are $n_w = n_{nw} = 2$.

Unless otherwise stated, $\kappa = 10^{-2}$, for all the cases, for the wetting phase and 0 for the non-wetting phase in Eq. (7). All remaining parameters for the test cases are provided in Table I.

In all test cases, the domain is initially saturated with the non-wetting phase at $(1 - S_{wirr})$. The wetting phase is injected through the left boundary, and flow is allowed to exit through the right boundary. The wetting phase is injected at a uniform constant velocity. On the outflow boundary, the pressure is set to 0.

Porosity and permeability are assumed homogeneous for the first and third cases (4.1 and 4.3). For case 4.2, the permeability is heterogeneous and isotropic; regions of constant $\mathbf{K}$ are considered. For cases 4.1 and 4.2, gravity effects are not considered. For case 4.3, gravity is acting in the vertical direction with a dimensionless acceleration of 1.

In the numerical experiments, three solution approaches are compared. The first is a simple FPMA ($\varphi = 1$), the second is FPMA with constant φ and no acceleration procedures (using the most efficient φ), and the third is adaptive φ with SFPI (with a maximum limit of nine iterations) and using acceleration with $\beta = 0.4$.

For the first test case (Section 4.1), the importance of using vanishing artificial diffusion is also tested. The total equivalent number of FPMAs is used as a comparison criterion. Regarding the

Table I. Model set-up for the test cases 4.1–4.3

	M^0	ϕ	$\mathbf{K}_1$	$\mathbf{K}_2$	S_{wirr}	S_{nwr}	$\Delta\rho$	u_{in}	Length	# ele
4.1	1	0.2	1.0	N/A	0.2	0.3	0	0.2	1.0	1400
4.2	5	0.2	1.0	1000	0.2	0.3	0	1.0	1.0	8655
4.3	1	0.2	1.0	N/A	0.2	0.3	0.289	1.0	1.0	9656

M^0 is the viscosity contrasts between the phases, and u_{in} is the inlet velocity.

DOI: 10.1002/fld

SFPI, as shown previously, each iteration requires one-third (computational time) of an FPMA, and therefore, it is considered as one-third in the total equivalent number of FPMA.

To check the convergence of the numerical simulations, the square of the L_2-norm of the size of the correction over all the nodes is tested:

$$f(S) = \sum_{i}^{N} \left(\frac{S'_k - S_{k_1}}{\varphi N} \right)_i^2, \tag{11}$$

where N is the total number of nodes. This criterion has been used previously for FPMA, especially for spiral-wise convergence, and it requires less computations than calculating the residual [20]. The solver iterates until the functional defined in Eq. (11) reaches the tolerance defined by the user, as shown in Figure 1 or the maximum number of FPMA is reached. The stopping criterion for the SPFI is the same as for the FPMA in terms of tolerance; however, the number of iterations is restricted as it may not be converging to the real solution, because the pressure is not updated. The FPMA (and SFPI) convergence criterion is to achieve an $f(S) = 10^{-9}$ for all the cases. To allow comparison of this convergence criterion with others based on using the residual, we find that achieving an $f(S) = 10^{-9}$ for the case 4.1 is equivalent to achieving an absolute residual of about 10^{-8}, measured using a normalized L_2-norm.

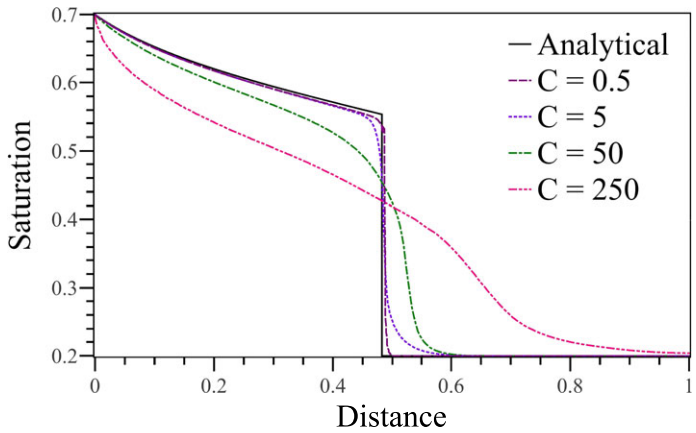

Figure 3. Saturation profile at the same point in time using different Courant numbers.

Table II. L_1 and L_2 errors using different Courant numbers.

Courant number	0.5	5.0	50	250
L_1	2.6×10^{-3}	5.63×10^{-3}	2.44×10^{-2}	7.86×10^{-2}
L_2	1.6×10^{-4}	2.32×10^{-3}	2.96×10^{-3}	5.62×10^{-3}

Table III. Average number of equivalent fixed point method of Anderson iterations per time step for different approaches and Courant numbers.

	$\varphi = 1$		φ Fixed		φ Adaptive accel.	
Courant number	$\kappa = 0$	$\kappa \neq 0$	$\kappa = 0$	$\kappa \neq 0$	$\kappa = 0$	$\kappa \neq 0$
0.5	2.0	2.0	2.0	2.0	2.0	2.0
5.0	N/A	> 500	15.3	9.0	10.0	4.7
50	N/A	N/A	145.8	40.0	47.4	13.0
250	N/A	N/A	> 500	59.5	289.0	29.0

DOI: 10.1002/fld

4.1. 1D immiscible displacement

In this test case, a non-wetting phase is displaced by a wetting phase generating a shock front that is moved through the domain. Pseudo 1D simulations are performed with four different Courant numbers to evaluate the performance of the method presented here. Figure 3 shows the 1D solutions compared with the semi-analytical solution (see [21] and Table II, the corresponding errors normalized by the number of nodes). As expected, as the Courant number is increased, the solution is more diffusive. Nonetheless, the behaviour of the system is well represented, and mass is conserved.

Table III shows that the inclusion of artificial diffusion of Eq. (7) proves to be very useful in order to reduce the number of FPMAs required to obtain convergence; however, backtracking techniques are necessary to obtain results with Courant numbers above 1. The dynamic calculation of φ together with the acceleration methods presented here improve the convergence of the FPMA solver, especially for large Courant numbers. Figure 4 shows the time series of number of equivalent FPMAs for three cases with a Courant number of 50. It can be seen that the use of over-relaxation stabilizes the solver and that the solution obtained using the method presented here is the most stable and converges faster.

4.2. 2D model of fractured rock domain

Here, a fracture model is considered. The fractures have very high permeability (1000 times higher than the surrounding matrix) and very high aspect ratio (width 1000 times smaller than the size of the model domain).

This model is designed to demonstrate that highly anisotropic meshes and large variations in material properties can be handled by the presented methodology. The mesh and the permeability map are shown in Figure 5(a). Three different experiments are compared. Table IV shows the FPMA necessary to convergence for different Courant numbers. Likewise, Figure 5(b–d) shows snapshots of the injected phase saturation at the same time for solutions obtained using the Courant numbers specified in Table IV. The behaviour of the model is consistent between different Courant numbers, introducing the injected phase preferentially through the highly permeable fractures, inside which the flow is effectively like in test case 4.1.

Compared with the previous model, here, the presented method proves to be much more useful as it is able to deal with Courant numbers up to 8600, while without this method, the solver cannot converge for Courant numbers above 5, which is very restrictive considering the very small elements (10^4 times smaller than the biggest element) appearing in the mesh.

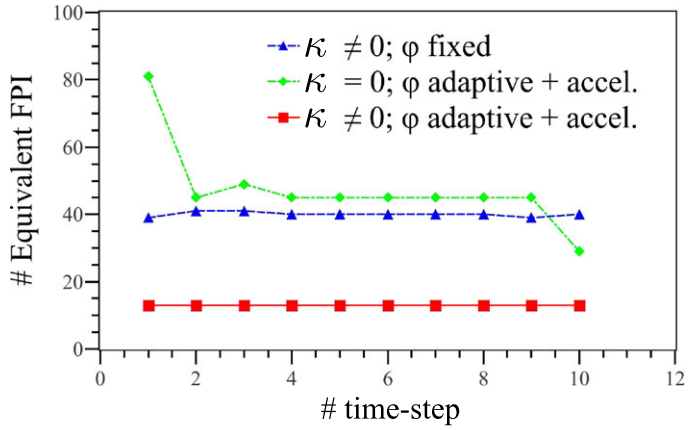

Figure 4. Number of equivalent fixed point methods of Anderson necessary to converge for three different configurations with a Courant number of 50. [Colour figure can be viewed at wileyonlinelibrary.com]

DOI: 10.1002/fld

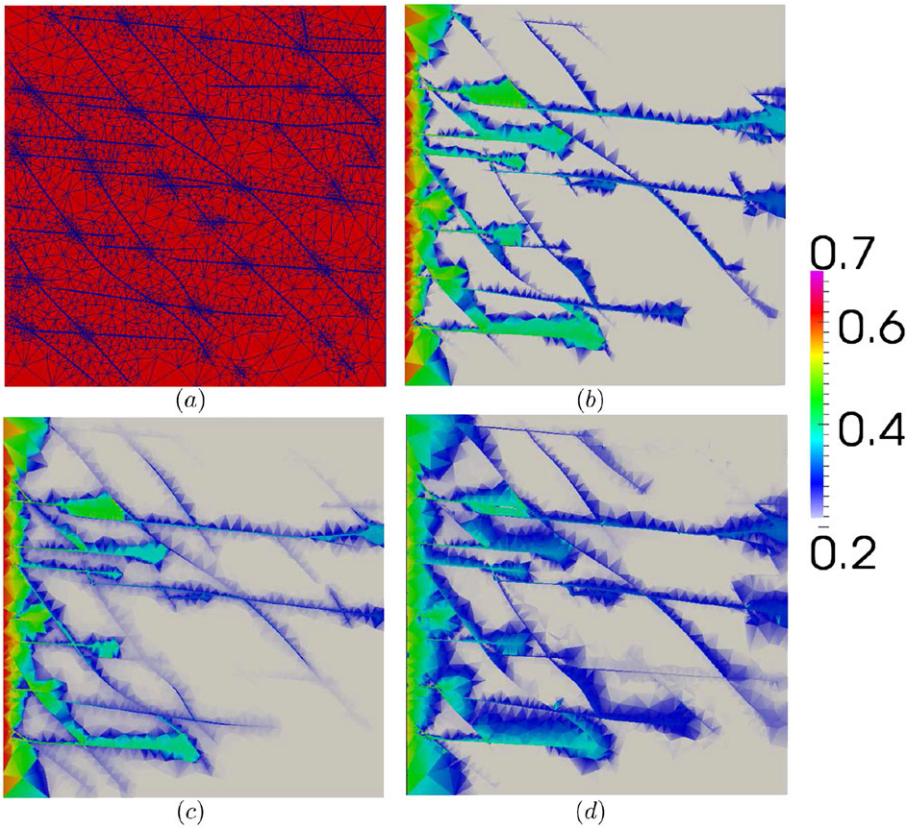

Figure 5. 2D model of fractures, from [22]. (a) Shows the permeability map plus the mesh used, composed of 8655 elements; (b), (c) and (d) show the injected phase saturation at the same time using different Courant numbers during injection into the left-hand face (following the same ordering used in Table V). [Colour figure can be viewed at wileyonlinelibrary.com]

Table IV. Average number of equivalent fixed point method of Anderson iterations per time step for different approaches and Courant numbers.

Courant number	$\varphi = 1$	φ Fixed	φ Adaptive accel.
5	2.0	2.0	2.0
215	N/A	N/A	3.33
8600	N/A	N/A	75

4.3. 3D model with gravity

In this section, a 3D displacement with gravity is considered. The inclusion of gravity is important as it adds another source of nonlinearity in the equations [5].

Figure 6 shows a snapshot of the injected phase saturation obtained using the methodology presented here and four different Courant numbers (0.5 (a), 5 (b), 50 (c) and 200 (d)). As expected, the behaviour is consistent, showing higher diffusion as the Courant number is increased but the same overall flow behaviour. In this case, the diffusion appears as a thicker 'tongue' of the injected phase. In Figure 6(b), the front is thicker, and the tip is retarded compared with (a); in Figure 6(c) and (d), the diffusion has expanded the front spanning the whole domain.

Table V shows that despite it being a 3D model including gravity, the presented method can achieve convergence in just 19 FPMA equivalent iterations for the case with the highest Courant number.

DOI: 10.1002/fld

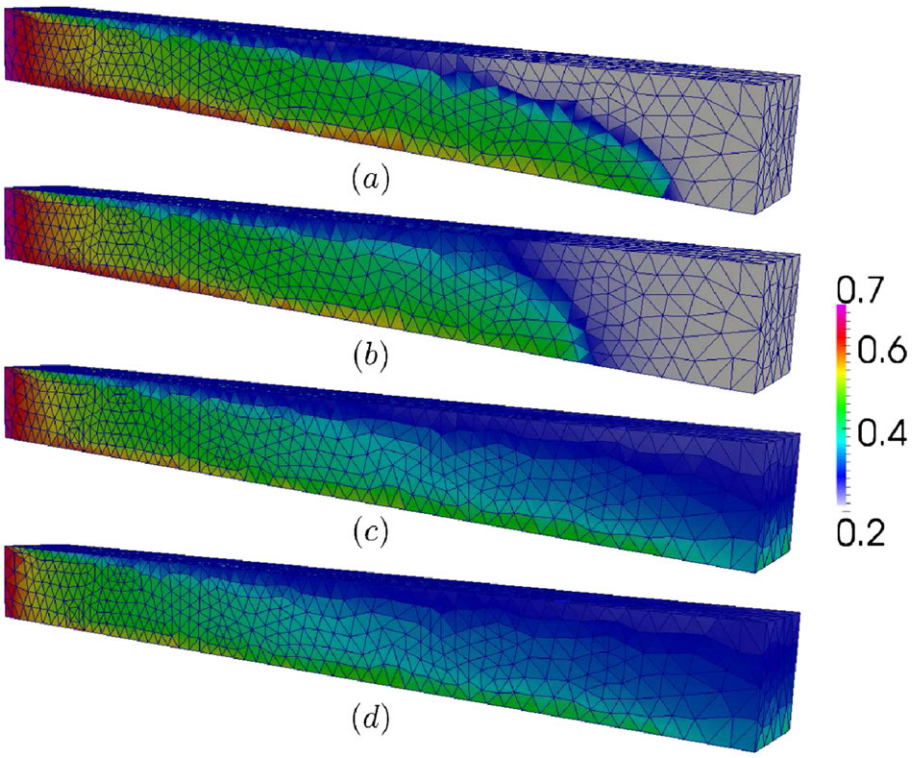

Figure 6. Saturation profile of the experiment shown in Table V at the same time using Courant numbers of 0.5 (a), 5 (b), 50 (c) and 200 (d). [Colour figure can be viewed at wileyonlinelibrary.com]

Table V. Average number of equivalent fixed point method of Anderson iterations per time step for different approaches and Courant numbers.

Courant number	$\varphi = 1$	φ Fixed	φ Adaptive accel.
0.5	2.0	2.0	2.0
5.0	2.0	2.0	2.0
50	N/A	20.5	12.0
200	N/A	31.5	19.0

5. CONCLUSIONS

An efficient and robust nonlinear solver with acceleration is presented. First, computational cost is reduced by adding a nested FPMA with a lower computational cost (approximately one-third of the conventional FPMA). Second, the convergence is improved by relaxing the saturation field after it is calculated, with the relaxation parameter calculated based only on the history of convergence. Third, the convergence rate is improved using a modification of Anderson's acceleration. Fourth, vanishing artificial diffusion is introduced in order to both aid the convergence and the convergence rate of the nonlinear solver. The method proposed is simple to implement and has been tested against different numerical simulations using a wide range of Courant numbers (up to 8600), showing it can achieve convergence rapid and robustly with respect to large Courant numbers.

ACKNOWLEDGEMENTS

Funding for Dr P. Salinas from ExxonMobil is gratefully acknowledged. Dr D. Pavlidis would like to acknowledge the support from the following research grants: Innovate UK Octopus, EPSRC Reactor Core-Structure Re-location Modelling for Severe Nuclear Accidents and Horizon 2020

DOI: 10.1002/fld

In-Vessel Melt Retention. Dr Z. Xie is supported by EPSRC ('Multi-Scale Exploration of Multiphase Physics in Flows' – MEMPHIS). Dr A. Adam acknowledges the funding from TOTAL. Part funding for Jackson under the TOTAL Chairs programme at Imperial College is also acknowledged. We also thank Qinghua Lei for providing the mesh and domain for the numerical experiment shown in Figure 5. More information about the AMCG group can be found in http://www.imperial.ac.uk/earth-science/research/research-groups/amcg/ and for the NORMS group here http://www.imperial.ac.uk/earth-science/research/research-groups/norms/.

REFERENCES

1. Jackson MD, Percival JR, Mostaghimi P, Tollit BS, Pavlidis D, Pain CC, Gomes JLMA, El-Sheikh AH, Salinas P, Muggeridge AH, Blunt MJ. Reservoir modeling for flow simulation by use of surfaces, adaptive unstructured meshes, and an overlapping-control-volume finite-element method. *SPE Reservoir Evaluation and Engineering* 2015; **18**. DOI: http://dx.doi.org/10.2118/163633-PA.
2. Salinas P, Percival JR, Pavlidis D, Xie Z, Gomes J, Pain CC, Jackson MD. A discontinuous overlapping control volume finite element method for multi-phase porous media flow using dynamic unstructured mesh optimization. *SPE 173279*, 2015.
3. Natvig JR, Lie K. Fast computation of multiphase flow in porous media by implicit discontinuous Galerkin schemes with optimal ordering of elements. *Journal of Computational physics* 2008.
4. Aziz K, Settari A. Petroleum Reservoir Simulation, Vol. 227, No.24. Applied Science Publishers, Academic Press Professional, Inc.: London, 2008; 10108–10124. DOI:10.1016/j.jcp.2008.08.024.
5. Li B, Tchelepi HA. Nonlinear analysis of multiphase transport in porous media in the presence of viscous, buoyancy, and capillary forces. *Journal of Computational Physics* 2015; **297**:104–131.
6. Anderson DG. Iterative procedures for nonlinear integral equations. *Journal of the Association Computational Machinery* 1965; **12**:547 –560.
7. Lott PA, Walker HF, Woodward CS, Yang UM. An accelerated fixed-point iteration for solution of variably saturated flow. *Advances in Water Resources* 2012; **38**:92 –101.
8. Gomes JLMA, Pavlidis D, Salinas P, Xie Z, Percival JR, Melnikova Y, Pain CC, Jackson MD. A force-balanced control volume finite element method for multiphase porous media flow modelling. *International Journal for Numerical Methods Fluids* 2016. DOI:10.1002/fld.4275, ISSN:1097–0363.
9. Atkinson KE. *An Introduction to Numerical Analysis*. Wiley, 2016. ISBN 0–471–62489–6.
10. Press WH, Teukolsky SA, Vetterling WT, Flannery BP. *Numerical Recipes: The Art of Scientific Computing*. Cambridge University Press: New York, 2007.
11. Sorensen DC. Newtons method with a model trust region modification. *SIAM Journal for Numerical and Analytical* 1982; **19**:409 –426.
12. Forsyth PA. A control volume, finite element method for local mesh refinement in thermal reservoir simulation. *SPE Resevoir Engineering* 1990; **5**(4):561–566.
13. Geiger S, Roberts S, Matthäi SK, Zoppou C, A. Burri A. Combining finite element and finite volume methods for efficient multiphase flow simulations in highly heterogeneous and structurally complex geologic media. *Geofluids* 2004; **4**(4):284–299.
14. Matthai SK, Mezentsev A, Belayneh M. Finite element-node centered finite-volume two-phase flow experiments with fractured rock represented by unstructured hybrid element meshes. *SPE* 2007; **93341**. DOI:http://dx.doi.org/10.2118/93341-PA.
15. Pavlidis D, Xie Z, Percival JR, Gomes JLMA, Pain CC, Matar O. Two- and three-phase horizontal slug flow modelling using an interface-capturing compositional approach. *International Journal for Multiphase Flow* 2014; **67**: 85–91.
16. Jenny P, Tchelepi HA, Lee SH. Unconditionally convergent nonlinear solver for hyperbolic conservation laws with s-shaped flux functions. *Journal of Computational Physics* 2009; **228**:7497 –7512.
17. Chen Zhangxin, Huan Guanren, Li Baoyan. An improved IMPES method for two-phase flow in porous media. *Transport in Porous Media* 2004; **54**(3):361–376. Available from: https://doi.org/10.1023/B.
18. Kelley CT. Iterative methods for linear and nonlinear equations 1995.
19. Brooks RH, Corey AT. *Hydrology Papers*, Vol. 3. SIAM, Colorado State University, 1964. ISBN: 978-0-898713-52-7.
20. Sterck HD, Ullrich P. *Introduction to Computational Mathematics*. University of Waterloo: Fort Collins, Colorado, 2006.
21. Buckley SE, Leverett MC. Mechanism of fluid displacements in sands. *Transactions of the AIME* 1942; **146**: 107–116.
22. Belayneh MW, Matthi SK, Blunt MJ, Rogers SF. Comparison of deterministic with stochastic fracture models in water-flooding numerical simulations. *AAPG Bulletin* 2009; **11**:1633–1648.